

# CHAOTIC ATTRACTORS WITH CYCLIC SYMMETRY REVISITED

KEVIN C. JONES

3329 25<sup>th</sup> Avenue, Moline IL 61265, U.S.A.  
*e-mail*: kjones15@uic.edu

CLIFFORD A. REITER

Department of Mathematics, Lafayette College, Easton PA 18042, U.S.A  
*e-mail*: reiterc@lafayette.edu  
(Preprint)

**Abstract**—Chaotic attractors generated by the iteration of polynomial functions with cyclic symmetry have been the subject of recent study. A new formulation is investigated which generates cyclic symmetry using arbitrary functions. This allows the use of diverse function classes including functions with various types of singularities. The resulting images have significantly more diversity than those arising from polynomials yet the cyclic symmetry of the chaotic attractor is preserved.

Keywords: chaos, symmetry, rotations, pattern

## 1. INTRODUCTION

The iteration of functions can lead to remarkable behaviors. Cayley confronted the intertwining basins of attraction of Newton's method long ago [6]. More recently, the Lorenz attractor that resulted from a model of weather [10] exhibits chaotic behavior was noted and that observation provoked many recent investigations involving chaos. Remarkably, chaotic behavior is not incompatible with symmetry. For example, snowflakes seem to contain a randomness suggestive of chaos while maintaining remarkable symmetry [2]. The juxtaposition of pattern with randomness and mixing have also been explored by artists. Escher made extensive use of symmetry with astonishing distortion [15] and Frank Stella creates art with remarkable patterns containing intriguing mixing and chaos [1, 17].

The study of attractors that are chaotic yet contain specified symmetry has been the subject of considerable study. Field and Golubitsky illustrate how to create chaotic attractors with symmetry in [9]. This work discusses cyclic and dihedral groups with their dramatic rotational symmetry. Other recent work on creating chaotic attractors with symmetry has been based on demanding that the coefficients of general polynomial or trigonometric functions satisfy certain criterion in order to respect the symmetry group of interest. This has included chaotic attractors with cubic [3], tetrahedral [12], hypercube [11], frieze and wallpaper [4,7] symmetries. However, in some cases, summing over the symmetry group in a special fashion has been useful as we will see. This idea was implicit in some of the wallpaper constructions in [9] and was used to create chaotic attractors with the symmetry of a dodecahedron in [13]. This summation can also be used with certain wallpaper groups which suggested methods for creating attractors near forbidden symmetry [8]. Other works involve attractors with delightful cyclic symmetry but are based upon graphics manipulations of attractors with other properties [5,14,16].

Illustrations in the literature describing chaotic attractors with cyclic and dihedral symmetry appear limited to the methods in [9] which are mainly polynomial based. By using the summation techniques described in the next section, we are able to broaden the investigation to

include other smooth functions which includes bump functions and trigonometric functions, as well as singular functions with fractional exponents and sawtooth discontinuities. In fact, the techniques we will investigate are so general that any type of function may be tried. The methods of [9] certainly yield visually interesting examples of chaotic attractors with cyclic symmetry, but we will be able to greatly expand the diversity of these illustrations.

## 2. FORMULATIONS

In order to obtain functions which produce chaotic attractors with symmetry, we seek classes of functions that have specified symmetry. We say a function  $f: \mathfrak{R}^2 \rightarrow \mathfrak{R}^2$  is *equivariant* with respect to a symmetry  $\sigma$  if  $f(\sigma(\bar{x})) = \sigma(f(\bar{x}))$  for all  $\bar{x} \in \mathfrak{R}^2$ . We think of a symmetry as a rigid motion that preserves distance – an isometry. In this note we are only concerned with cyclic and dihedral symmetry groups. The cyclic group  $C_n$  is generated by  $n$ -fold rotations about a single point. The dihedral group  $D_n$  contains those rotations and a reflection through a line passing through the point of rotation. The equivariance condition implies  $f^n(\sigma(\bar{x})) = \sigma(f^n(\bar{x}))$ . Thus, if  $\sigma$  is a rotation, the rotations of the iterates of  $f$  must be the same as the iterates of the rotation. It is possible that attractors arising from such functions will only visit restricted regions and conjugate attractors are needed to see the complete expected symmetry; moreover, the attractor can, and often does, degenerate. Nonetheless, such equivariant functions  $f$  are good places to seek attractors with the desired symmetry.

Field and Golubitsky [9] determine classes of functions which are equivariant with respect to  $C_n$  and  $D_n$ . In particular, they prove that all the polynomial functions  $f: \mathfrak{R}^2 \rightarrow \mathfrak{R}^2$  that are equivariant with respect to the dihedral group  $D_n$  or the cyclic group  $C_n$  have a particular form. They focus on a special case. Namely, if  $\alpha, \beta, \gamma, \omega$  are real parameters, they define

$$f(z) = (\lambda + \alpha z \bar{z} + \beta \operatorname{Re}(z^n) + \omega i)z + \gamma \bar{z}^{n-1}$$

where  $z = x + iy$  is the complex variable corresponding to the point  $(x, y)$  in the plane. This function  $f(z)$  is equivariant with respect to  $C_n$  and when  $\omega = 0$  then it is equivariant with respect to  $D_n$ . They also consider some illustrations with a singularity at the origin using a similar function that utilizes an additional real parameter  $\delta$  and an integer  $p$ :

$$g(z) = \left( \lambda + \alpha z \bar{z} + \beta \operatorname{Re}(z^n) + \delta \operatorname{Re}\left(\left(\frac{z}{|z|}\right)^{np}\right) |z| \right) z + \gamma \bar{z}^{n-1}.$$

Figure 1 shows an image with  $C_6$  symmetry created using a function of the form  $f(z)$ . Color in the image corresponds to the frequency with which the corresponding pixel was visited. Points visited no times are white. Those visited a small number of times are cyan, and those visited the most times are violet and yellow. The rapidness of color change is determined according to a logarithmic bias on the frequency table. The figure illustrates the desired symmetry; and while there are six “windows” where the probability of hitting is much lower than for other parts of the attractor, there is an overall smoothness and coherence.

Our technique for creating chaotic attractors with these symmetries is quite different. We make use of the following fact. We state the result for the plane, but the result is true in any dimension [13].

**Proposition 1:** Let  $P: \mathfrak{R}^2 \rightarrow \mathfrak{R}^2$  be an arbitrary function and let  $G$  be a finite group realized by 2 by 2 matrices acting on  $\mathfrak{R}^2$  by multiplication on the right, and define

$$f_{P,G}(\vec{x}) = \sum_{\sigma \in G} \sigma^{-1}(P(\sigma(\vec{x})))$$

Then  $f_{P,G}(\vec{x})$  is equivariant with respect to  $G$ .

*Proof:* Let  $\gamma \in G$ . Then

$$f_{P,G}(\gamma(\vec{x})) = \sum_{\sigma \in G} \gamma(\sigma\gamma)^{-1}(P(\sigma(\gamma(\vec{x})))) = \gamma\left(\sum_{\sigma \in G} (\sigma\gamma)^{-1}(P((\sigma\gamma)(\vec{x})))\right) = \gamma(f_{P,G}(\vec{x}))$$

by the linearity of  $\gamma$  and the fact that  $\sigma\gamma$  runs through  $G$  as  $\sigma$  does.  $\square$

We next turn to describing the particular representations of  $C_n$  and  $D_n$  which we will use

in Proposition 1. Let  $R_n = \begin{pmatrix} \cos\left(\frac{2\pi}{n}\right) & -\sin\left(\frac{2\pi}{n}\right) \\ \sin\left(\frac{2\pi}{n}\right) & \cos\left(\frac{2\pi}{n}\right) \end{pmatrix}$  and  $S = \begin{pmatrix} 1 & 0 \\ 0 & -1 \end{pmatrix}$ . The matrix  $R_n$  is the

generator of an  $n$ -fold rotation and hence  $\{R_n^i | 0 \leq i \leq n-1\}$  is a realization of  $C_n$ . We will consider  $C_n$  to be equal to that set of matrices. Likewise, the matrix  $S$  is a mirror through the first coordinate and hence we consider  $D_n = \{R_n^i | 0 \leq i \leq n-1\} \cup \{SR_n^i | 0 \leq i \leq n-1\}$ . Thus, we will investigate the creation of cyclic and dihedral symmetry using functions  $f(x)$  of the form of the Proposition, with  $G = C_n$  or  $G = D_n$ . We vary the arbitrary function  $P(x)$  to include classes of polynomial, trigonometric, bump, fractional power and mod 1 functions.

### 3. EXPERIMENTS

We begin with illustrations arising from the functions that are the smoothest and most comparable to the classical construction [9]. First, we create polynomials  $R: \mathfrak{R}^2 \rightarrow \mathfrak{R}^2$ . The  $k^{\text{th}}$  output coordinate of  $R(\vec{x})$  is given by  $R(\vec{x})_k = \sum_{\substack{0 \leq i \leq 2 \\ 0 \leq j \leq 2}} a_{ijk} x_0^i x_1^j$  where  $0 \leq k \leq 2$  and  $\vec{x} = \langle x_0, x_1 \rangle$ . Thus, our function is

specified by the three dimensional array  $a_{ijk}$  of parameters where  $i$  corresponds to the power of the first coordinate,  $j$  corresponds to the power of the second coordinate and  $k$  specifies the output coordinate. For any choice of that parameter array,  $f_{R,G}(\vec{x})$  as defined in Proposition 1 will be equivariant with respect to the symmetry group  $G$ .

Figure 2 shows an example of a function created in this way using the symmetry group  $D_5$ . This group of symmetries contains a reflection and a rotation of  $2\pi/5$  radians around the origin. In order to locate visually interesting attractors with this symmetry, we select the entries for the three dimensional array  $a_{ijk}$  randomly between -1 and 1. After taking the sum of conjugates over the symmetry group, we test the resulting function for a Ljapunov exponent indicative of chaos and create an image if the test is positive. Visually attractive images located that way are then run at higher resolution. In Figure 2, points hit by the function a small number of times are colored yellow, points hit the most number of times are colored blue, and those hit an intermediate number of times are colored green, violet, or red.

The appendix contains the J code for constructing the function used to create Figure 2. At <http://www.lafayette.edu/~reiterc/j> a more complete script may be found. It gives all the functions used in this paper and sample steps to create images. Links to downloading the language J may also be found there.

Second, we create trigonometric functions  $T: \mathfrak{R}^2 \rightarrow \mathfrak{R}^2$ . The  $i^{\text{th}}$  output coordinate of  $T(\vec{x})$  is given by  $T(\vec{x})_i = \sum_{1 \leq k \leq 3} a_{i0k} \sin(kx_i) + a_{i1k} \cos(kx_i)$  where  $0 \leq i \leq 1$ . Thus, our function is determined by the three dimensional array  $a_{ijk}$  where  $i$  specifies the output coordinate,  $j$  corresponds to the choice between sin and cos, and  $k$  specifies the frequency multiplier. Notice these trigonometric functions don't have any mixing of coordinates. However, the sum of conjugates from Proposition 1 will introduce mixing.

Figure 3 and Figure 4 are generated by the sum of conjugates of trigonometric functions of this form as in Proposition 1. The groups  $C_7$  and  $D_5$  are used in the creating the functions whose attractors are shown in Figures 3 and 4, respectively. Note that the attractor in Figure 3 approaches  $D_{14}$  near the center, while Figure 4 has intriguing concentric arches.

We next focus on functions containing products of trigonometric terms  $S: \mathfrak{R}^2 \rightarrow \mathfrak{R}^2$ . To simplify the notation, we will set  $f_1(x) = \cos(2x)$ ,  $f_2(x) = \sin(x)$ , and  $f_3(x) = \sin(2x)$ . Then the  $k$ -th coordinate of  $S(\vec{x})$  is given by  $S(\vec{x})_k = \sum_{\substack{0 \leq i \leq 2 \\ 0 \leq j \leq 2}} a_{ijk} f_i(x_0) f_j(x_1)$  where  $0 \leq k \leq 2$  and  $\vec{x} = \langle x_0, x_1 \rangle$ .

These functions will give products of trigonometric terms instead of sums, and will mix coordinates even before using the sum of conjugates from Proposition 1.

The attractor in Figure 5 was created using a sum of conjugates of  $S(\vec{x})$  with  $D_6$  as the group of symmetries. A palette was chosen especially to highlight the slight difference in frequency in areas that are only hit a small number of times by the function. The oscillations highlighted in magenta illustrate a qualitative behavior that seems to arise with low but dependable frequency when products of the trigonometric terms appear.

Third we create bump functions  $B: \mathfrak{R}^2 \rightarrow \mathfrak{R}^2$ . The  $i^{\text{th}}$  output coordinate of  $B(\vec{x})$  is given by  $B(\vec{x})_i = \sum_{0 \leq j \leq 2} a_{ij} e^{-2(x_i - j/2)^2}$  where  $0 \leq i \leq 1$ . Thus, this function is determined by the two dimensional array  $a_{ij}$  where  $i$  gives the output coordinate and  $j$  corresponds to the position of a bump in the bump function.

In Figure 6 the attractor is the result of a bump function summed over the symmetries in  $D_3$ . Here, the areas hit by the function the least are colored yellow, and the areas hit the most are colored red and purple. Note that the densest areas are in bands at different distances from the origin.

Fourth, we create fractional power functions  $F: \mathfrak{R}^2 \rightarrow \mathfrak{R}^2$ . The 0 and 1 output coordinates of  $F(\vec{x})$  are given by  $F(\vec{x})_0 = \sum_{0 \leq j \leq 2} a_{j0} \operatorname{Re}(w_j)$  and  $F(\vec{x})_1 = \sum_{0 \leq j \leq 2} a_{j1} \operatorname{Im}(w_j)$  where  $w_j = (x + iy)^{1/(2j+3)}$ . Thus, this complex fractional power function is determined by the two dimensional array  $a_{jk}$  where  $k$  corresponds to the real and imaginary parts of the fractional powers, and  $j$  corresponds to changing the fractional power.

The attractors in Figures 7 and 8 are the result of sums of conjugates of fractional power functions conjugated using the symmetries of  $D_3$ . It is interesting to note that in Figure 7, the "holes" in the attractor are eight-pointed. Figure 7 appears to be made out of polygons in contrast with the earlier, smoother figures. It is also worthwhile to point out that in Figure 8, the attractor appears to have an additional distorted similarity which might be called an annular glide reflection. Notice that the outermost components resemble hats with a figure-like component beneath them. Notice that upon a sixth of a turn around the origin, the innermost component seems to resemble that hat with a figure-like component but the direction from the origin is inverted. The resulting

symmetry is similar to  $D_3$ -enhanced p1a1 symmetry described in [5]. Further study may reveal reasons for this unexpected behavior.

Lastly, we create functions  $Q: \mathfrak{R}^2 \rightarrow \mathfrak{R}^2$  which are polynomial functions reduced mod 1. That is,  $Q(\bar{x}) = R(\bar{x}) \bmod 1$ . Thus, such functions are determined by a three dimensional array  $a_{ijk}$  where  $i$  corresponds to the power of  $x_0$ ,  $j$  corresponds to the power of  $x_1$  and  $k$  specifies the output coordinate.

Figures 9 and 10 are generated by sums of polynomials mod 1 using the symmetries of  $C_3$  and  $C_4$ , respectively. Even though the polynomials mod 1 have discontinuities, these figures have the required symmetry and include what appear to be many overlapping components. Sometimes these components are arranged in somewhat parallel configurations leading to feathery or spiral-like images. In Figure 10, a black background is chosen to highlight the relatively thin attractor more effectively.

#### 4. CONCLUSION

We have investigated a new technique for creating cyclic symmetry in the presence of chaos: summing over the conjugates by the symmetries in a group. This technique is so general that arbitrary functions can be used to create new functions with the desired cyclic or dihedral symmetry. Using polynomials, trigonometric functions, exponential bump functions, fractional complex exponential functions, and polynomials mod 1 results in qualitatively different attractors. Since the underlying functions may have properties of their own, additional distorted similarities may also arise. With the new technique we are able to create aesthetically pleasing images with greater diversity and additional interesting structure.

*Acknowledgment* — This work was supported by DMS-9805507. We appreciate the use of code by the authors of [4] for the creation of Figure 1.

#### APPENDIX

The following J code creates the function that is used to generate the attractor shown in Figure 2. At <http://www.lafayette.edu/~reiterc/j> a complete script giving all the functions used in this paper and sample steps to create images may be found.

```

Prods=: \:~@~. @ (* >&1e_14@:|) @ ( , ( , / ) @ : ( ( + / . * "2) / ~ ) )
sin=: 1&o.
cos=: 2&o.
rotn=: (cos, -@sin) , : (sin, cos)
cd=: Prods^: _ @ : (rotn@+: @o. @% , : 1 0 "_ , : 0 : , *)

consum=: 2 : 0
x=: + / . *
+/@((% . n.) "_ x" 2 1 ] ) @ : (u. "1) @ (n. &x) f.
)

P=: 1 : 0
x=: + / . *
(1&{ x 0&{ x m. "_ ) @ (^ / &(i.3))
)

```

```

p02=:3 3 2$, ".;._2]0 : 0
0.111601 _0.327589
0.215598 _0.452505
_0.253271 0.274297
0.113096 _0.198432
_0.0450232 0.295369
0.267113 0.368732
0.275252 0.160737
_0.488431 _0.0672858
0.127573 0.111203
)

s02=:_5

f02=: (p02 P) consum (cd s02)

]f02^(i.5) 0.1 0.2
0.1 0.2
_0.1684 _0.337103
0.280257 0.558578
_0.444799 _0.905096
0.662754 1.22628

```

The function builder `consum` takes a function and a group of symmetries as argument and creates a new function using the sum of conjugates as in Proposition 1. The function builder `P` creates the polynomial from our set of parameters, `p02`. Here, `cd` generates the symmetries of the group  $D_5$ , and `f02` is the sum of the conjugates of our initial function `p02 P` over the symmetry group. The first four iterations of the function are then presented which is useful for comparison with alternate implementations.

## REFERENCES

1. Axsom, R. A., *The Prints of Frank Stella*. Hudson Hills Press, New York, 1983.
2. Bentley, W. A. and Humpherys, W. J., *Snow Crystals*. Dover Publications, Inc., New York, 1962.
3. Brisson, G., Gartz, K., McCune, B., O'Brien, K. and Reiter, C., Symmetric attractors in three-dimensional space. *Chaos, Solitons & Fractals*, 1996, **7** (7), 1033-1051.
4. Carter, N., Eagles, R., Grimes, S., Hahn, A., and Reiter C., Chaotic attractors with discrete planar symmetries. *Chaos, Solitons & Fractals*, 1998, **9** (12), 2031-2054.
5. Carter, N., Grimes, S. and Reiter, C., Frieze and Wallpaper Chaotic Attractors with a Polar Spin. *Computers & Graphics*, 1998, **22** (6) 765-779.
6. Cayley, The Newton-Fourieir Imaginary Problem. *American Journal of Mathematics*, 1879, **2**, 97.
7. Dumont, J., Heiss, F., Jones, K., Reiter, C. and Vislocky, L., Chaotic attractors and evolving planar symmetry. *Computers & Graphics*, to appear.
8. Dumont, J. and Reiter, C., Chaotic attractors near forbidden symmetry. *Chaos, Solitons & Fractals*, to appear.

9. Field M. and Golubitsky, M., *Symmetry in Chaos*. Oxford University Press, New York, 1992.
10. Lorenz, E. N., Deterministic nonperiodic flow. *Journal of Atmosphere Science*, 1963, **20**, 13-141.
11. Reiter, C., Attractors with the symmetry of the  $n$ -cube. *Experimental Mathematics*, 1996, **5** (4) 327-336.
12. Reiter, C., Chaotic attractors with the symmetry of the tetrahedron. *Computers & Graphics*, 1997, **21** (6) 841-848.
13. Reiter, C., Chaotic attractors with the symmetry of the dodecahedron. *The Visual Computer*, to appear.
14. Reiter, C., Attractors with dueling symmetry. *Computers & Graphics*, 1997, **21** (2) 263-271.
15. Schattsneider, D., *Visions of Symmetry: Notebooks, Periodic Drawings and related Work of M.C.Escher*. Freeman, New York, 1990.
16. Sprott, J. C. Strange attractor symmetric icons. *Computers & Graphics*, 1996, **20** (2) 325-332.
17. Stella, F., *Frank Stella, Moby Dick Series*, Cantz, Ostfildern-Ruit bei Stuttgart, 1993.

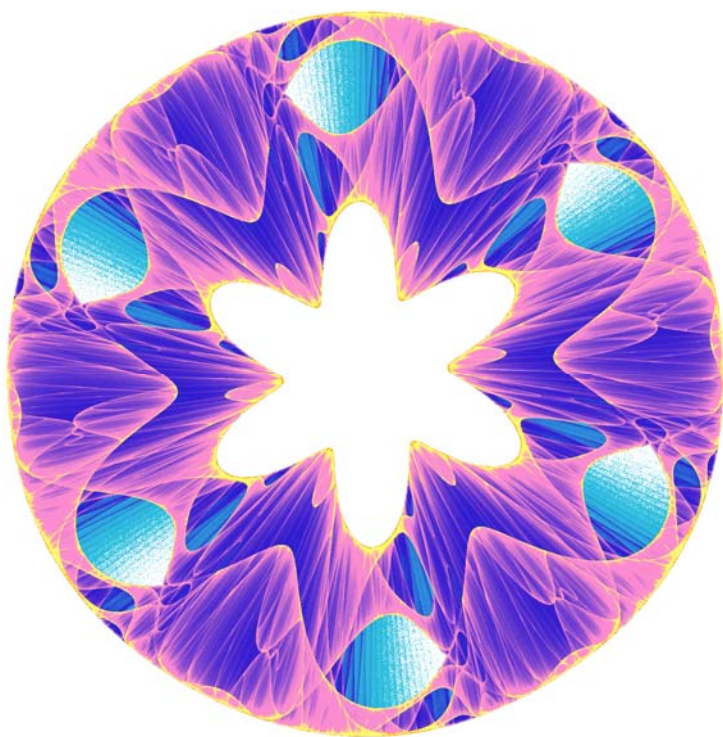


Fig 1. An attractor with  $C_6$  symmetry.

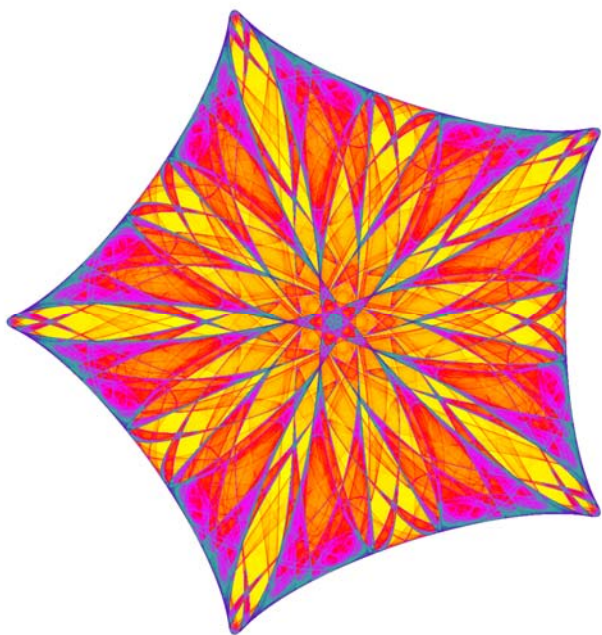


Fig 2. An attractor with  $D_5$  symmetry generated with polynomials.

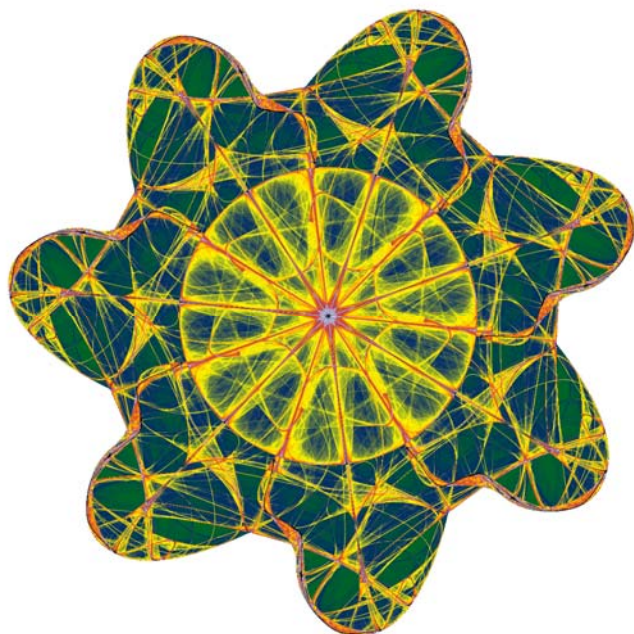


Fig 3. An attractor with  $C_7$  symmetry generated with trigonometric sums.

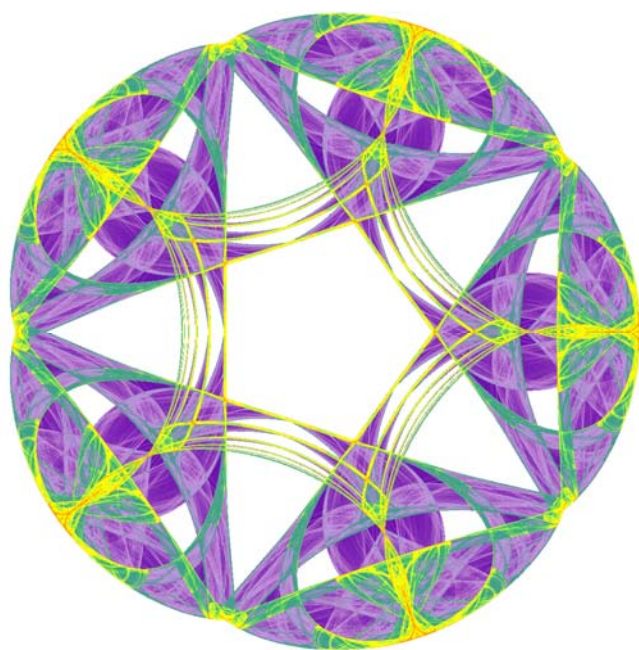


Fig 4. An attractor with  $D_5$  symmetry generated with trigonometric sums.

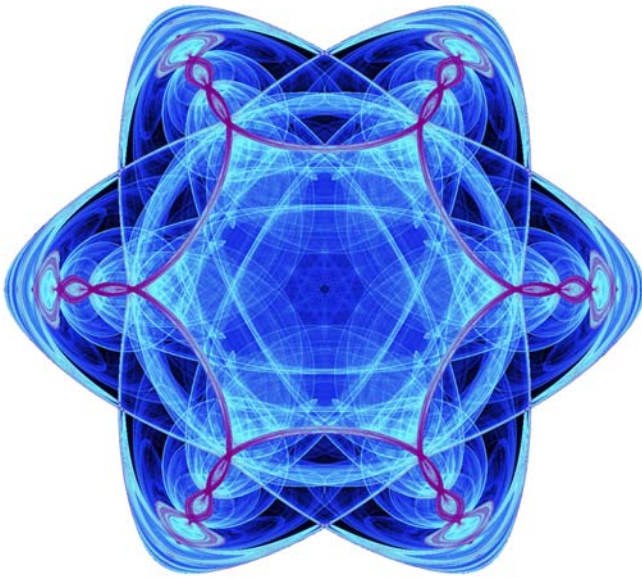


Fig 5. An attractor with  $D_6$  symmetry generated with sums of trigonometric products.

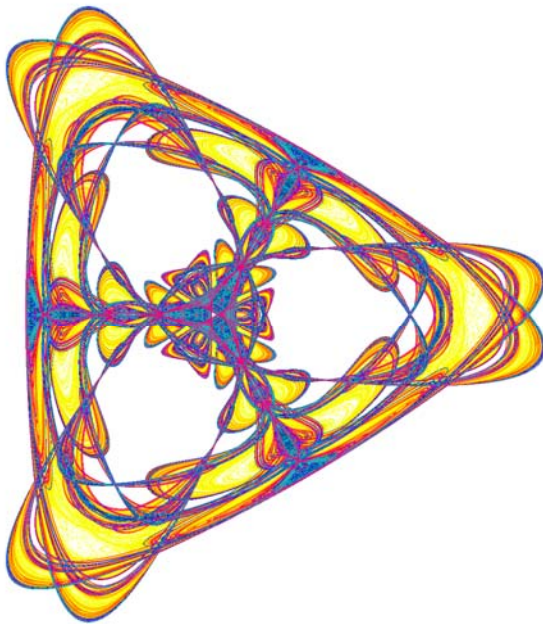


Fig 6. An attractor with  $D_3$  symmetry generated with a bump function.

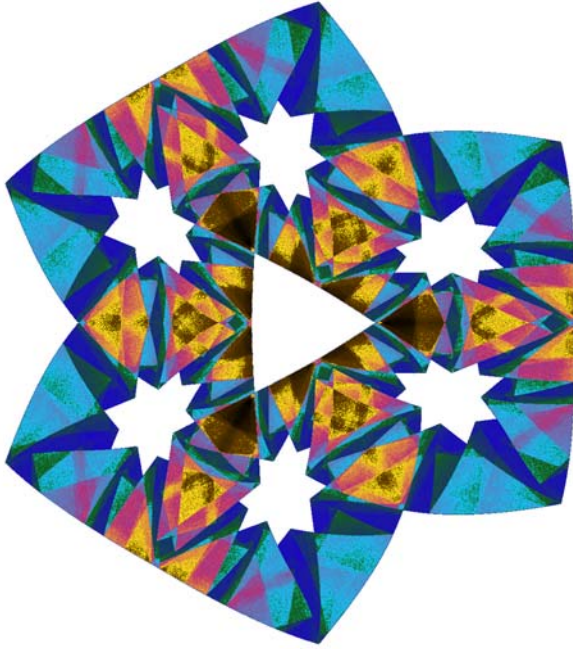


Fig 7. An attractor with  $D_3$  symmetry generated by a fractional power function.

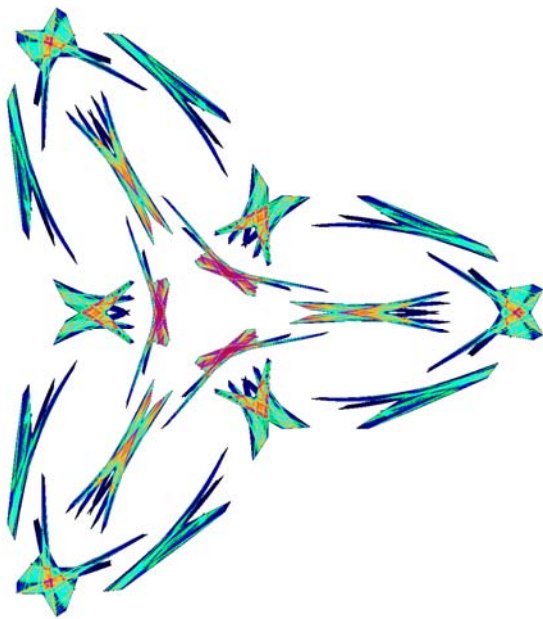


Fig 8. An attractor with  $D_3$  symmetry generated by a fractional power function with a distorted glide reflection.

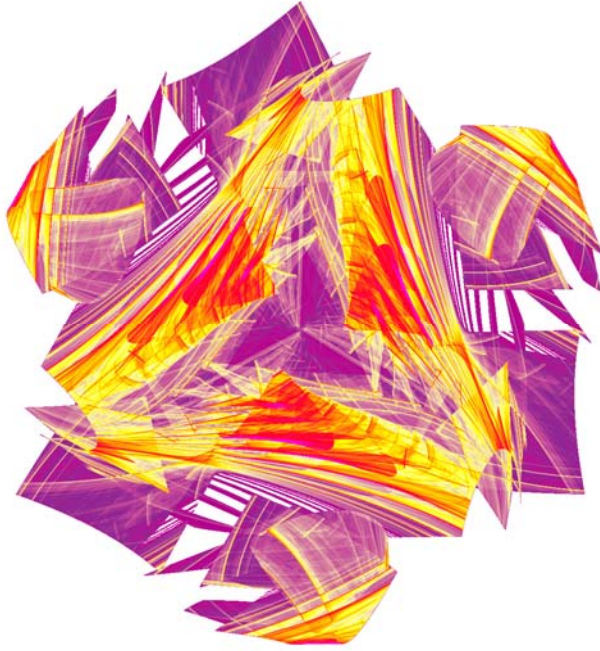


Fig 9. An attractor with  $C_3$  symmetry generated by polynomials mod 1.

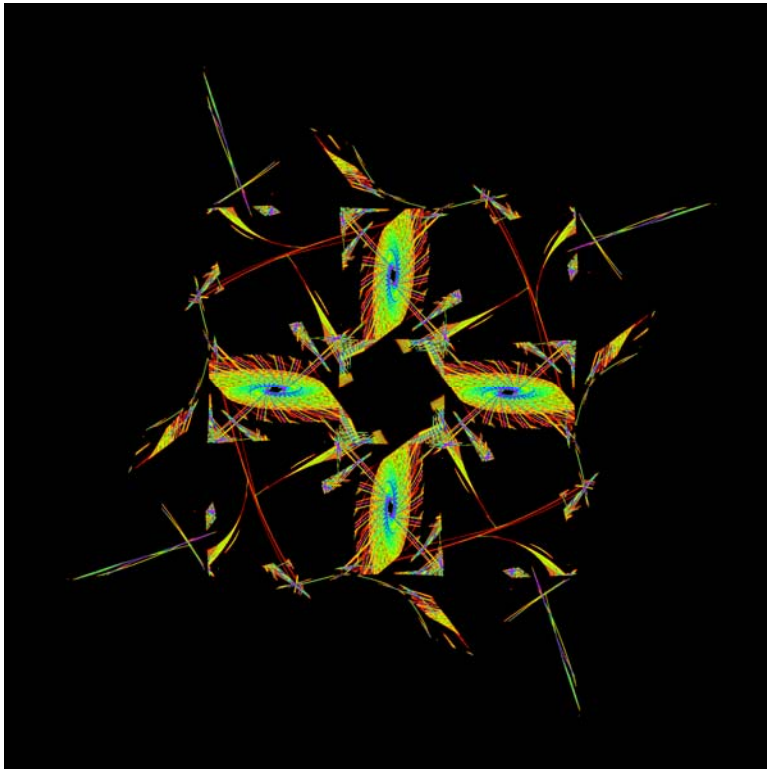


Fig 10. An attractor with  $C_4$  symmetry generated by polynomials mod 1.